Chemical Equilibrium Modeling and Experimental Measurement of Solubility for Friedel's Salt in the Na–OH–Cl–NO3–H2O Systems up to 200 °C

ARTICLE *in* INDUSTRIAL & ENGINEERING CHEMISTRY RESEARCH · AUGUST 2010

Impact Factor: 2.59 · DOI: 10.1021/ie101028c

2 AUTHORS:

Jiayu Ma
Wuhan Institute of Technology
6 PUBLICATIONS **36** CITATIONS
SEE PROFILE

Zhibao Li
Chinese Academy of Sciences
67 PUBLICATIONS **604** CITATIONS
SEE PROFILE

Chemical Equilibrium Modeling and Experimental Measurement of Solubility for Friedel's Salt in the Na−OH−Cl−NO_3−H_2O Systems up to 200 °C

Jiayu Ma and Zhibao Li*

Key Laboratory of Green Process and Engineering, Institute of Process Engineering, National Engineering Laboratory for Hydrometallurgical Cleaner Production Technology, Chinese Academy of Sciences, Beijing 100190, People's Republic of China

A chemical model for the solubility of Friedel's salt (FS, $3CaO\cdot Al_2O_3\cdot CaCl_2\cdot 10H_2O$) was developed. The model was built with the help of the OLI platform via regression of experimental solubility data for FS in the Na−OH−Cl−NO_3−H_2O systems. The solubility of FS in water was measured using a batch nickel autoclave over the temperature range of 20−200 °C, and the solubility product of FS ($\log_{10} K_{sp}$) was obtained. It was found that the solubility of FS in water shows a maximum value as a function of temperature. The solubility of FS in 0−5 mol/L NaOH and 0−2.5 mol/L NaCl solutions was found to decrease with increasing NaOH and NaCl concentrations, because of the common ion effect; however, in 0−2.5 mol/L $NaNO_3$ solutions, it was found to increase because of complexation. During the regression analysis, it was found that $CaOH^+$ plays an important role in solubility modeling, and its dissociation constant was determined by an empirical equation. New Bromley−Zemaitis activity coefficient model parameters for the Ca^{2+}−OH^-, $CaOH^+$−OH^-, and $CaCl^+$−OH^- ion pairs were also regressed, using the experimental solubility data generated in the present study. The new model was shown to successfully predict the solubility of FS in mixed NaOH + $NaNO_3$ solutions not used in model parametrization. With the aid of the newly developed model, the concentration and temperature effects on calcium species distribution were analyzed.

1. Introduction

Silica is one of the main impurities in bauxite.[1] The presence of silica in bauxite can cause caustic and aluminum loss during digestion, scale buildup of heat exchangers, and product quality issues.[2−4] Therefore, desilication is indispensable in the alumina industry. Most recently, Friedel's salt ($3CaO\cdot Al_2O_3\cdot CaCl_2\cdot 10H_2O$, abbreviated as FS), belonging to the layered double hydroxide family,[5] was proved by the authors[6] to have higher desilication capacity than conventional desilication agents, such as calcium oxide or calcium hydroxide. Furthermore, FS can be prepared using calcium chloride generated from the soda ash industry and used a desilication agent instead of calcium oxide or calcium hydroxide in the alumina industry. To understand the desilication behavior and mechanism of FS in alkaline solutions, it is necessary to know the solubility of FS in alkaline solutions. The effect of some impurities, i.e., NaCl, $NaNO_3$, etc., on the solubility of FS in alkaline solutions also should be considered.

Besides desilication, FS recently attracted much attention because of its ion exchange characteristic.[5] For example, FS can be applied in the disposal of radioactive, hazardous, and mixed wastes.[7−9] Walcarius et al.[10] reported that FS is used as a novel electrode modifier for the accumulation of iodide species. Qian et al.[11] found that FS can strongly fix heavy metals from electronic sludge wastes. Dai et al.[12] examined the adsorption behaviors of FS for Cr(VI) from aqueous solutions at different concentrations and various initial pH values. However, in some processes, such as removal of Cr(VI) or fixation of heavy metals from aqueous solutions using FS, the pH values of aqueous solutions also need to be considered. Therefore, the knowledge of the solubility of FS at different pH values is essential.

Chemical modeling of aqueous electrolyte solutions is becoming increasingly important in the development, analysis, design, and control of chemical and hydrometallurgical processes. Chemical modeling works in acidic media or neutral solutions have been intensively described in the open literature. Azimi, Papangelakis, and Dutrizac[13−17] developed a model to predict successfully calcium sulfate solubilities in acidic media including HCl and H_2SO_4. Li and Demopoulos[18,19] used the Bromley−Zemaitis activity coefficient model[20] to estimate successfully the solubility of calcium sulfate in HCl and in HCl-based aqueous solutions containing various metal chloride salts over the temperature range of 10−100 °C. More recently, Cheng and Li[21] proposed a model with the help of the OLI platform to calculate accurately the supersaturation of $Mg_5(CO_3)_4(OH)_2\cdot 4H_2O$ in the $MgCl_2$−Na_2CO_3 system in supersaturated solutions over the temperature range of 50−90 °C. Most of the previous studies have been focused on the prediction work in acidic media. However, the modeling works in alkaline media are very limited.

The purpose of the present work is to develop, with the aid of the OLI platform, a chemical equilibrium model to estimate the solubility of FS in the Na−OH−Cl−NO_3−H_2O systems. To be concrete, the solubility of FS in the Na−OH−Cl−NO_3−H_2O systems or at different pH values was determined by the isothermal dissolution method. The solubility product parameters of FS were obtained by the regression of the solubility data in H_2O at various temperatures and then were added into a new databank. With this new databank, OLI gave poor estimation results, with regard to the solubility of FS in the Na−OH−Cl−NO_3−H_2O systems. To improve OLI's solubility estimation capacity, new model parameters, such as Bromley−Zemaitis parameters for the Ca^{2+}−OH^-, $CaOH^+$−OH^-, and $CaCl^+$−OH^- ion pairs and empirical dissociation constant parameters of $CaOH^+$, were determined by the regression of the solubility data of FS in H_2O and in single electrolyte solutions. The new model parameters were tested against the

* To whom correspondence should be addressed. Tel.: +86-10-62551557. Fax: +86-10-62551557. E-mail: zhibaoli@home.ipe.ac.cn.

10.1021/ie101028c
Published on Web 08/26/2010

solubility of FS in mixed NaOH + $NaNO_3$ solutions not used in model parametrization. Finally, the newly developed model was used to analyze the concentration and temperature effects on calcium species distribution.

2. Experimental Section

2.1. Experimental Materials. Analytically pure HCl, NaOH, $Al(OH)_3$, NaCl, and $NaNO_3$ were supplied by Beijing Chemical Plant with minimum purities of 36.5%−38.0%, 98.0%, 98.5%, 99.5%, and 99.0%, respectively. $CaCl_2$ (99.0%) was supplied by Sinopharm Chemical Reagent Co. Ltd. All solutions used in this study were prepared by dissolving analytical-grade chemicals directly without further purification. Distilled water with specific conductivity of 0.1 μS/cm was used. The initial pH between 1 and 12 was adjusted by dilute HCl or NaOH solution, and its exact value was determined by the pH meter (KANGYI pH meter, PHS-25C).

2.2. Preparation and Characterization of FS. Preparation of Friedel's salt (FS) was performed in a 1-L glass mixed-tank reactor. The reactor was stirred with a Teflon impeller driven by a multivariable speed motor under autocontrolled agitation, where the heating oil circulates from a thermostat batch to precisely control the temperature within ±0.1 °C. Preparation experiments were conducted by preheating 0.5 M $CaCl_2$ (300 mL) to 80 °C and adding an equal volume of 0.25 M $NaAlO_2$ solution (α_k = 3.2) at a rate of 5 mL/min using a peristaltic pump, while stirring at 300 rpm. When the addition procedure was completed, stirring continued for 4 h. The white precipitate then was collected, filtered off, washed with distilled water three times (to remove any possible ionic remnants), and finally dried in an oven at 50 °C for 10 h. The structure and morphology of the synthesized samples were examined using powder X-ray diffraction (XRD) and scanning electron microscopy (SEM) (JEOL Model JSM-6700F). Powder XRD (X'Pert PRO MPD, PANalytical, Almelo, The Netherlands) patterns were recorded on a diffractometer (using Cu Kα radiation) operating at 40 kV/30 mA. A scanning rate of 0.02°/s was applied to record the patterns in the 2θ angle range of 5°−90°.

2.3. Measurement of Solubility. The approaches that determine the solubility of salts in solutions can be categorized as either the dissolution method or the precipitation method.[22] The dissolution method is considered to be more reliable and feasible, because it avoids the complication of formation of intermediate phases that is commonly encountered in precipitation. In this work, the dissolution method was used.

The solubility of FS in H_2O was carried out in a 1-L nickel autoclave, manufactured by the XINYUAN Chemical Instrument Company of Weihai (China). Agitation was provided by a motor-driven titanium shaft impeller. Temperature was controlled by manipulating an electrical heating mantle and a cooling water stream, maintaining the autoclave temperature within ±1 °C of the set point. The autoclave was equipped with a dip tube for sample withdrawal through an in situ 2-μm porous ceramic filter. A volume of 600 mL of H_2O was placed in the autoclave with excess solid (5 g of FS). Experiments were started by heating the autoclave to a certain temperature and allowing sufficient time (10 h) to reach equilibrium. Samples of 50 mL were taken at a prescribed time and filtered immediately. The liquor was analyzed for Ca by titration with ethylenediaminetetraacetic acid (EDTA). The solid phase was filtered and washed three times with distilled water. The washed solids were dried at 50 °C for 12 h and then analyzed by powder XRD to determine whether the solid phase had been altered by phase transformation. In addition, SEM imaging techniques were also used for examination of the solid phases.

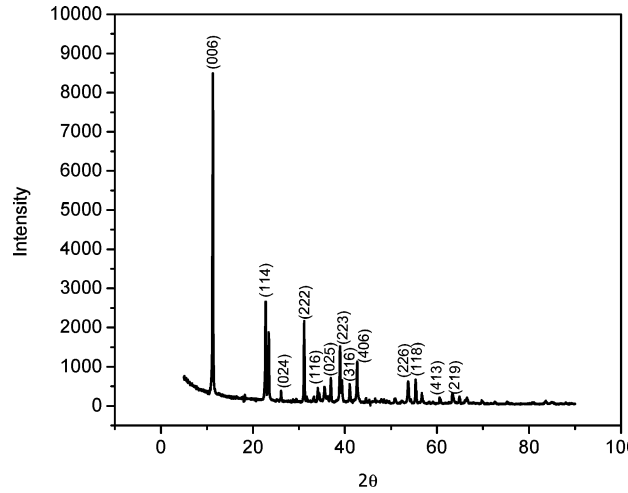

Figure 1. X-ray diffraction (XRD) pattern of Friedel's salt (FS) prepared at 80 °C.

The solubility of FS in salt solutions under atmospheric pressure was determined inside a 250-mL glass bottle where heating was provided through a temperature-controlled water bath. To summarize, the 200 mL of salt solution of known composition with FS solids was introduced into a glass bottle thermostated at a selected temperature with constant magnetic stirring. The temperature was controlled to ±0.1 °C. Ten hours of contact time was used to ensure the equilibration between FS and solutions. After equilibration, the clear solution was sampled and filtered to measure the solution density at the temperature of the system. Next, the calcium content of filtered FS saturated solution was analyzed by titration with EDTA to determine the solubility. The solubility (s) was expressed as molality (mol/kg H_2O). Finally, the washed and dried solid phases were examined by XRD to determine whether the solid phase had been altered due to phase transformation during equilibration.

To verify the reproducibility and accuracy of the adopted procedure in this work, several experiments were carried out. The average deviation of the determined solubility of FS in water at 100 °C was within ±0.00012 mol·dm^{-3}, with a relative deviation of 2.8%. Three replicate measurements of FS solubility in 1 mol·dm^{-3} NaOH at 50 °C were also carried out; the average deviation was ±0.00008 mol·dm^{-3}, with a relative deviation of 3.7%.

3. Results and Discussion

3.1. Purity and Morphology of FS. Figure 1 displays the XRD pattern of FS synthesized at 80 °C. All peaks in the XRD pattern were in good agreement with the FS literature values (Joint Committee on Powder Diffraction Standards (JCPDS) File Card No. 78-2051). Figure 2 shows typical SEM images of flat hexagonal (or pseudo-hexagonal) crystal morphology with some aggregation and nonuniform growths observed.

The purity of FS was determined via the chemical titration method. FS (5 g) was dissolved in an excess of low-concentration (~0.1 M) hydrochloric acid solution. The concentration of Ca^{2+} ions in the solution was determined by titration, using EDTA solution with an error of <0.5%. The results showed that the purity of the FS sample synthesized in this study was 99.1%, which satisfies the requirement of solubility measurements.

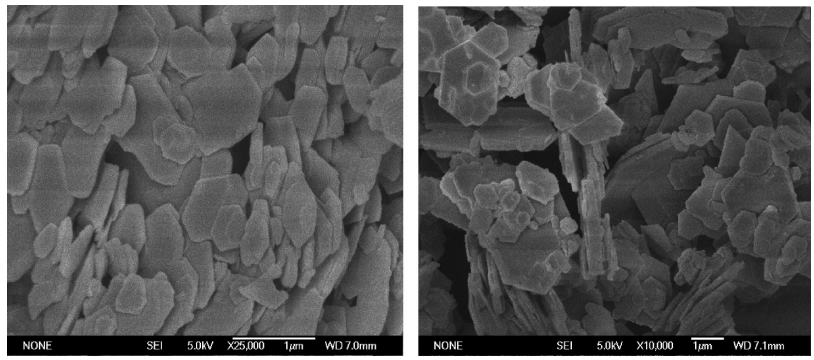

Figure 2. Scanning electron microscopy (SEM) morphologies of FS prepared at 80 °C.

Table 1. Solubility of FS (1) in H_2O (2) (Equilibration Time = 10 h)

	Solubility as $3CaO \cdot Al_2O_3 \cdot CaCl_2$ in Different Units		
temperature (°C)	C_1 (g/L)	M_1 (mol/L)	m_1 (mol/kg)
20	1.29525	0.00340	0.00343
25	1.36095	0.00357	0.00360
30	1.44344	0.00379	0.00382
35	1.67311	0.00439	0.00442
40	1.85285	0.00486	0.00489
45	1.92748	0.00506	0.00509
50	1.95902	0.00514	0.00519
55	2.02621	0.00532	0.00534
60	2.13206	0.00560	0.00561
65	2.17272	0.00570	0.00574
70	2.20921	0.00580	0.00582
80	2.04236	0.00562	0.00565
90	1.95929	0.00514	0.00532
100	1.76262	0.00463	0.00483
110	1.60024	0.00420	0.00442
130	1.06368	0.00279	0.00299
150	0.66266	0.00174	0.00190
170	0.35996	0.00094	0.00105
190	0.17222	0.00045	0.00052
200	0.11797	0.00031	0.00036

3.2. Solubility of FS in the Na−OH−Cl−NO_3−H_2O Systems. 3.2.1. FS−H_2O System. FS solubility in water was measured in the temperature range of 20−200 °C. The results of experimentally determined solubility are summarized in Table 1 and demonstrated graphically in Figure 3. In Table 1, the solubility of FS was expressed both in molarity (M or mol·L^{-1}) and molality (m or mol·kg^{-1}) for convenient practical and thermodynamic reference. As can be seen from Figure 3, the solubility of FS initially increases to a maximum value and then

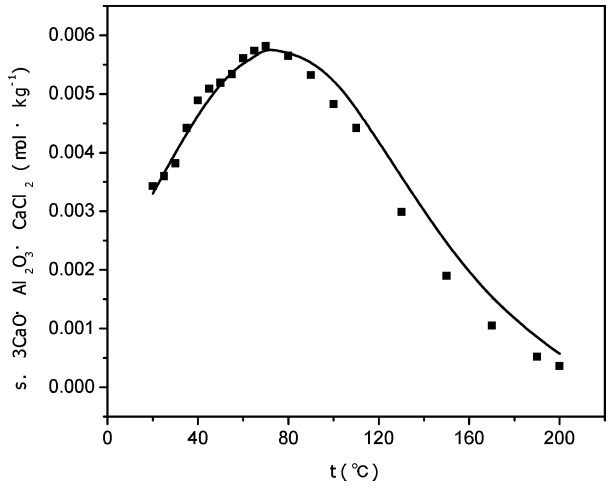

Figure 3. Solubility of FS in water at different temperatures. Points represent experimental data; the curve represents the fitted model.

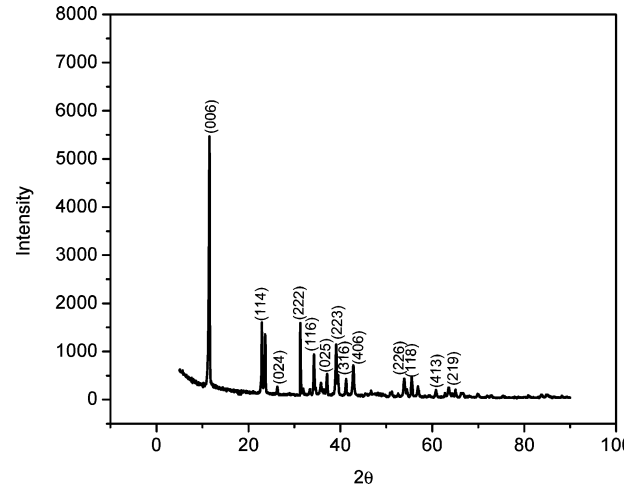

Figure 4. XRD pattern of FS in water after 10 h at 200 °C.

decreases gradually with an increase of the temperature above ~80 °C. The XRD analysis of equilibrated solid phases (Figure 4) showed that FS is stable in water up to 200 °C, and the same deduction was also verified by the SEM images, as shown in Figure 5.

3.2.2. FS−NaOH−H_2O System. In the present work, the solubility of FS in aqueous NaOH systems was measured at 30−70 °C. Table 2 and Figure 6 summarize the experimental data for FS in this system. As can be seen, the solubility of FS increases with increasing temperature but first decreases sharply with increasing NaOH concentration, because of the common ion effect of added OH^- and then rather slowly with increasing NaOH concentration above 1 mol/kg. The solubility increase is attributable to the increase of the K_{sp} of FS as the temperature increases from 30 °C to 70 °C. The XRD study in Table 7 (shown later in this paper) shows that FS is stable within the temperature range of 30−70 °C in NaOH solutions with concentrations up to 5 mol/L.

3.2.3. FS−NaCl−H_2O System. The solubility of FS at 30, 50, and 70 °C in NaCl solutions with concentrations up to 2.5 mol/L was determined using the same procedure. The results determined in this study are given in Table 3 and demonstrated graphically in Figure 7. As can be seen, the solubility of FS in this system increases with increasing temperature but decreases with increasing NaCl concentration, because of the common ion effect of added Cl^-. XRD analysis (see results in Table 7, presented later in this work) shows that FS is stable over the temperature range of 30−70 °C.

3.2.4. FS−$NaNO_3$−H_2O System. The same approach was used to obtain the solubility of FS in 0.1−2.5 mol/L $NaNO_3$ solutions at 30, 50, and 70 °C. The results of experimentally

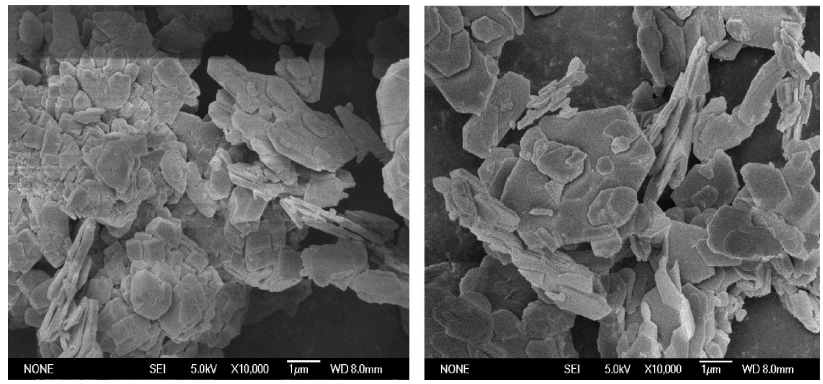

Figure 5. SEM morphologies of FS in water after 10 h at 200 °C.

Table 2. Solubility of FS (1) in NaOH (2) + H_2O (3) (Equilibration Time = 10 h)

Solution Parameters			Solubility as $3CaO \cdot Al_2O_3 \cdot CaCl_2$ in Different Units		
M_2 (mol/L)	m_2 (mol/kg)	ρ_s (g/mL)	C_1 (g/L)	M_1 (mol/L)	m_1 (mol/kg)
			T = 30 °C		
0.100	0.1006	0.9984	0.7184	0.00188	0.00189
0.500	0.5070	1.0156	0.4500	0.00118	0.00116
1.000	1.0254	1.0306	0.3793	0.00099	0.00096
1.500	1.5572	1.0544	0.3125	0.00082	0.00078
2.000	2.1039	1.0736	0.2970	0.00078	0.00073
2.500	2.6665	1.0944	0.2873	0.00075	0.00069
3.000	3.2464	1.1084	0.2796	0.00073	0.00066
3.500	3.8447	1.1256	0.2749	0.00072	0.00064
4.000	4.4628	1.1440	0.2633	0.00069	0.00060
4.500	5.1029	1.1616	0.2461	0.00064	0.00055
5.000	5.7657	1.1760	0.2258	0.00059	0.00050
			T = 50 °C		
0.100	0.1014	0.9992	1.0079	0.00265	0.00265
0.500	0.5111	1.0162	0.6759	0.00177	0.00175
1.000	1.0340	1.0388	0.5283	0.00139	0.00134
1.500	1.5708	1.0566	0.4416	0.00116	0.00110
2.000	2.1225	1.0746	0.4147	0.00109	0.00101
2.500	2.6906	1.0951	0.3571	0.00094	0.00086
3.000	3.2765	1.1092	0.3436	0.00090	0.00081
3.500	3.8813	1.1264	0.3347	0.00088	0.00078
4.000	4.5070	1.1480	0.3289	0.00086	0.00075
4.500	5.1549	1.1623	0.3228	0.00085	0.00073
5.000	5.8261	1.1768	0.3183	0.00084	0.00071
			T = 70 °C		
0.100	0.1024	0.9998	1.1331	0.00297	0.00298
0.500	0.5164	1.0178	0.7894	0.00207	0.00204
1.000	1.0450	1.0412	0.6224	0.00163	0.00157
1.500	1.5876	1.0578	0.5259	0.00138	0.00131
2.000	2.1452	1.0765	0.4536	0.00119	0.00111
2.500	2.7196	1.0962	0.4335	0.00114	0.00104
3.000	3.3120	1.1102	0.4179	0.00110	0.00099
3.500	3.9235	1.1285	0.3938	0.00103	0.00092
4.000	4.5563	1.1496	0.3513	0.00092	0.00080
4.500	5.2117	1.1635	0.3497	0.00092	0.00079
5.000	5.8921	1.1785	0.3439	0.00090	0.00077

determined solubility are listed in Table 4 and demonstrated graphically in Figure 8. As can be seen, the solubility of FS increases with increasing temperature and $NaNO_3$ concentration, because of the association of Ca^{2+} and NO_3^- ions and the formation of calcium nitrate complexes.[23,24] The XRD analysis of the equilibrated solids for this system is summarized in Table 7 (presented later in this paper). It can be observed that FS is stable at 30−70 °C, up to 2.5 mol/L $NaNO_3$.

3.2.5. FS−NaOH−$NaNO_3$−H_2O System. The solubility of FS in a mixture of 0.1−1.0 mol/L NaOH and 0.1−2.0 mol/L $NaNO_3$ was obtained at 30 °C. The results of experimentally determined solubility are listed in Table 5 and demonstrated graphically in Figure 9. As can be seen, the solubility of FS

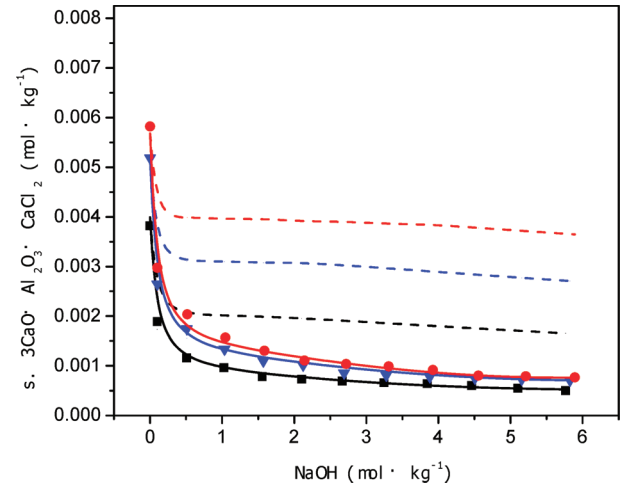

Figure 6. Solubility of FS in NaOH solutions: (■) 30 °C, (▲) 50 °C, and (●) 70 °C. Points present experimental data; the dashed lines are the estimation values using default databank of OLI; the solid lines are the regressed values.

increases with increasing $NaNO_3$ concentration but decreases with increasing NaOH concentration. The XRD study in Table 7 (shown later in this paper) shows that FS is stable in the NaOH−$NaNO_3$−H_2O system at 30 °C.

3.3. Solubility of FS at Various pH Values. Figure 10 presents the measured solubility data for FS as a function of

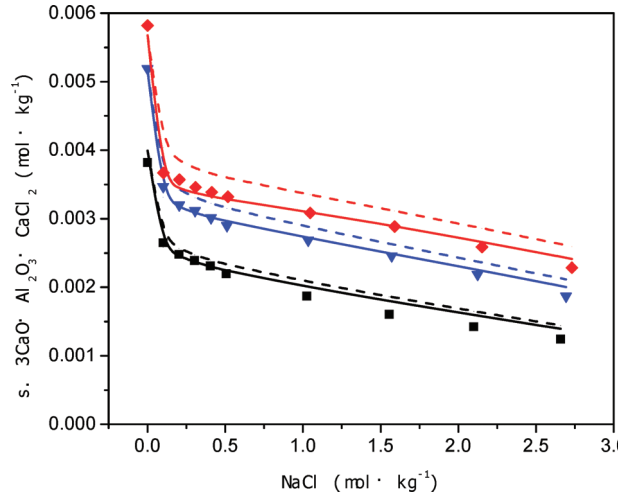

Figure 7. Solubility of FS in NaCl solutions: (■) 30 °C, (▲) 50 °C, and (●) 70 °C. Points present experimental data; the dashed lines are the estimated values using the default databank of OLI; the solid lines are the regressed values.

Table 3. Solubility of FS (1) in NaCl (2) + H_2O (3) (Equilibration Time = 10 h)

Solution Parameters			Solubility as $3CaO \cdot Al_2O_3 \cdot CaCl_2$ in Different Units		
M_2 (mol/L)	m_2 (mol/kg)	ρ_s (g/mL)	C_1 (g/L)	M_1 (mol/L)	m_1 (mol/kg)
		$T = 30$ °C			
0.100	0.1006	0.9996	1.0091	0.00265	0.00265
0.200	0.2017	1.0023	0.9469	0.00249	0.00248
0.300	0.3031	1.0078	0.9176	0.00241	0.00239
0.400	0.4049	1.0125	0.8910	0.00234	0.00231
0.500	0.5071	1.0152	0.8887	0.00233	0.00230
1.000	1.0257	1.0336	0.7749	0.00203	0.00197
1.500	1.5556	1.0528	0.7227	0.00190	0.00180
2.000	2.0997	1.0700	0.6208	0.00163	0.00152
2.500	2.6592	1.0908	0.5577	0.00146	0.00134
		$T = 50$ °C			
0.100	0.1014	1.0016	1.3232	0.00347	0.00347
0.200	0.2032	1.0035	1.2236	0.00321	0.00320
0.300	0.3054	1.0098	1.2259	0.00322	0.00319
0.400	0.4082	1.0135	1.2015	0.00315	0.00311
0.500	0.5114	1.0156	1.1599	0.00304	0.00300
1.000	1.0348	1.0346	1.0980	0.00288	0.00279
1.500	1.5719	1.0568	0.9887	0.00260	0.00246
2.000	2.1245	1.0723	0.9338	0.00245	0.00229
2.500	2.6941	1.0923	0.8189	0.00215	0.00197
		$T = 70$ °C			
0.100	0.1025	1.0025	1.4007	0.00368	0.00367
0.200	0.2053	1.0042	1.3392	0.00351	0.00350
0.300	0.3087	1.0113	1.3321	0.00350	0.00346
0.400	0.4125	1.0142	1.3085	0.00343	0.00339
0.500	0.5168	1.0161	1.2862	0.00338	0.00332
1.000	1.0465	1.0358	1.2571	0.00330	0.00319
1.500	1.5909	1.0586	1.2041	0.00316	0.00299
2.000	2.1517	1.0735	1.0988	0.00288	0.00269
2.500	2.7309	1.0934	0.9934	0.00261	0.00239

Table 4. Solubility of FS (1) in $NaNO_3$ (2) + H_2O (3) (Equilibration Time = 10 h)

Solution Parameters			Solubility as $3CaO \cdot Al_2O_3 \cdot CaCl_2$ in Different Units		
M_2 (mol/L)	m_2 (mol/kg)	ρ_s (g/mL)	C_1 (g/L)	M_1 (mol/L)	m_1 (mol/kg)
		$T = 30$ °C			
0.100	0.1005	1.0040	1.8731	0.004916	0.004898
0.200	0.2011	1.0080	2.0993	0.005510	0.005468
0.300	0.3018	1.0130	2.2671	0.005950	0.005876
0.400	0.4026	1.0180	2.3980	0.006294	0.006185
0.500	0.5036	1.0220	2.4748	0.006495	0.006358
1.000	1.0112	1.0468	2.8536	0.007490	0.007158
1.500	1.5251	1.0724	3.2084	0.008421	0.007856
2.000	2.0467	1.0928	3.3526	0.008799	0.008056
2.500	2.5780	1.1200	3.5307	0.009267	0.008278
		$T = 50$ °C			
0.100	0.1013	1.0044	2.3174	0.006082	0.006058
0.200	0.2027	1.0103	2.5695	0.006744	0.006678
0.300	0.3043	1.0156	2.7454	0.007206	0.007098
0.400	0.4063	1.0195	2.8956	0.007600	0.007458
0.500	0.5083	1.0280	3.0583	0.008027	0.007812
1.000	1.0229	1.0476	3.6135	0.009484	0.009058
1.500	1.5457	1.0756	4.0076	0.010519	0.009785
2.000	2.0781	1.0935	4.2158	0.011065	0.010125
2.500	2.6215	1.1268	4.4565	0.011697	0.010387
		$T = 70$ °C			
0.100	0.1023	1.0048	2.4790	0.006507	0.006478
0.200	0.2049	1.0135	2.7362	0.007182	0.007089
0.300	0.3078	1.0168	2.9774	0.007815	0.007689
0.400	0.4110	1.0205	3.1308	0.008217	0.008056
0.500	0.5150	1.0288	3.3086	0.008684	0.008445
1.000	1.0379	1.0489	3.8690	0.010155	0.009687
1.500	1.5714	1.0768	4.2551	0.011168	0.010387
2.000	2.1162	1.0964	4.4586	0.011702	0.010680
2.500	2.6734	1.1286	4.6797	0.012283	0.010890

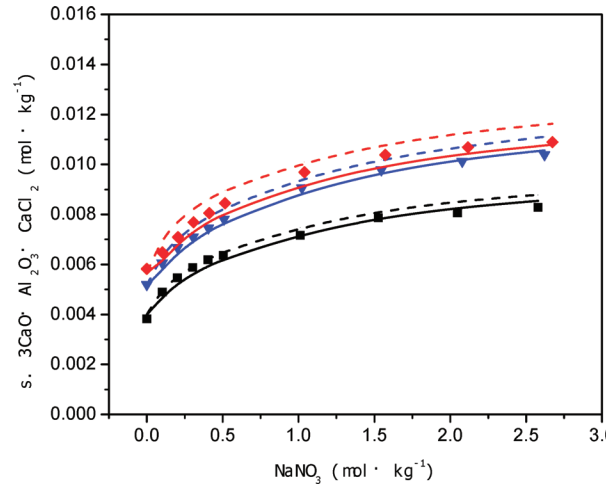

Figure 8. Solubility of FS in $NaNO_3$ solutions: (■) 30 °C, (▲) 50 °C, and (●) 70 °C. Points represent experimental data, the dashed lines represent the estimated values using the default databank of OLI, the solid lines represent the regressed values.

Table 5. Solubility of FS (1) in NaOH (2) + $NaNO_3$ (3) + H_2O (4) at 30 °C (Equilibration Time = 10 h)

Solution Parameters					Solubility as $3CaO \cdot Al_2O_3 \cdot CaCl_2$ in Different Units		
M_2 (mol/L)	M_3 (mol/L)	m_2 (mol/kg)	m_3 (mol/kg)	ρ_s (g/mL)	C_1 (g/L)	M_1 (mol/L)	m_1 (mol/kg)
0.09962	0.100	0.1004	0.1007	1.0029	0.6896	0.001810	0.001827
0.09962	0.500	0.1017	0.5104	1.0232	1.0401	0.002730	0.002795
0.09962	1.000	0.1036	1.0395	1.0478	1.2344	0.003240	0.003379
0.09962	2.000	0.1079	2.1689	1.0979	1.4402	0.003780	0.004091
0.49810	0.100	0.5020	0.1008	1.0168	0.4107	0.001078	0.001091
0.49810	0.500	0.5092	0.5111	1.0365	0.4903	0.001287	0.001321
0.49810	1.000	0.5189	1.0417	1.0555	0.5852	0.001536	0.001616
0.49810	2.000	0.5411	2.1728	1.1122	0.6816	0.001789	0.001940
0.9962	0.100	1.0060	0.1010	1.0370	0.3143	0.000825	0.000834
0.9962	0.500	1.0210	0.5124	1.0590	0.3760	0.000987	0.001011
0.9962	1.000	1.0411	1.0451	1.0820	0.4058	0.001065	0.001113
0.9962	2.000	1.0873	2.1828	1.1321	0.4397	0.001154	0.001253

pH at different temperatures. Table 6 lists the measured solubility values for FS at various pH values and temperatures. As can be seen from Figure 10, the solubility decreases sharply at pH values from 1 to 3 and then decreases smoothly with

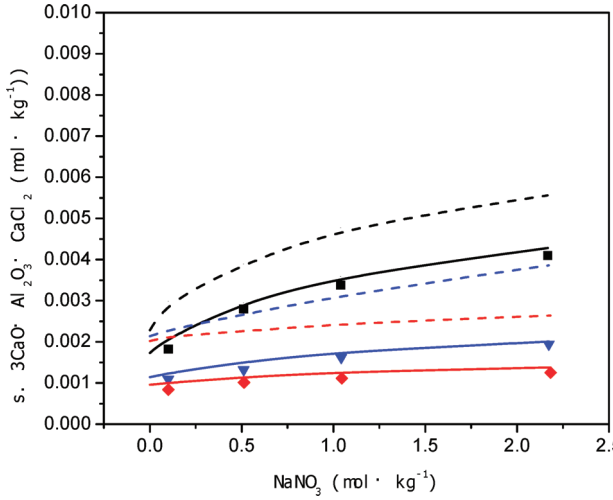

Figure 9. Solubility of FS in NaOH + $NaNO_3$ mixed solutions at 30 °C: (■) in 0.1 M NaOH, (▲) in 0.5 M NaOH, and (●) in 1.0 M NaOH. Points represent experimental data, the dashed lines represent the estimated values using the default databank of OLI, and the solid lines represent the values predicted by the obtained parameters.

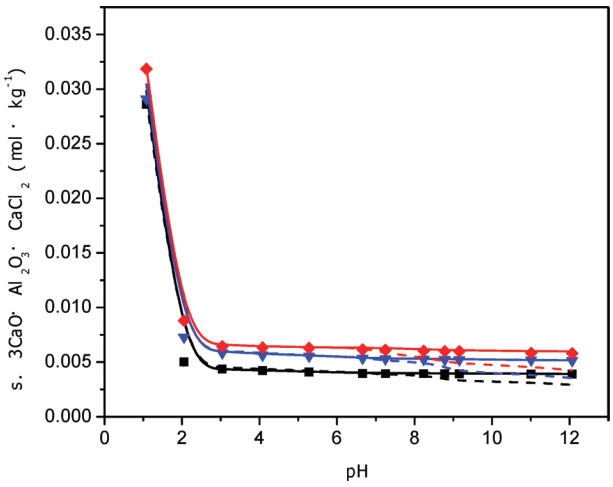

Figure 10. Solubility of FS at various pH values: (■) 30 °C, (▲) 50 °C, and (●) 70 °C. Points represent experimental data, the dashed lines represent the estimation values using the default databank of OLI, and the solid lines represent the values predicted by the parameters obtained.

Table 6. Solubility of FS (1) at Various pH Values (Equilibration Time = 10 h)

Solution Parameters		Solubility as $3CaO \cdot Al_2O_3 \cdot CaCl_2$ in Different Units		
pH	ρ_s (g/mL)	C_1 (g/L)	M_1 (mol/L)	m_1 (mol/kg)
		$T = 30$ °C		
1.08	0.9976	10.8591	0.028502	0.028600
2.05	0.9916	1.6960	0.004452	0.004490
3.04	0.9924	1.6014	0.004203	0.004236
4.08	0.9916	1.5620	0.004100	0.004135
5.28	0.9948	1.5484	0.004064	0.004086
6.66	0.9956	1.5019	0.003942	0.003960
7.25	0.9918	1.4848	0.003897	0.003930
8.24	0.9944	1.4882	0.003906	0.003929
8.78	0.9952	1.4880	0.003906	0.003925
9.16	0.9952	1.4865	0.003902	0.003921
11.01	0.9928	1.4727	0.003865	0.003894
12.07	0.9908	1.4663	0.003849	0.003885
		$T = 50$ °C		
1.08	0.9988	11.0620	0.029034	0.029100
2.05	0.9916	2.3135	0.006072	0.006125
3.04	0.9932	2.2102	0.005801	0.005842
4.08	0.9940	2.1363	0.005607	0.005642
5.28	0.9948	2.0997	0.005511	0.005541
6.66	0.9956	2.0305	0.005329	0.005354
7.25	0.9936	2.0011	0.005252	0.005287
8.24	0.9968	1.9900	0.005223	0.005241
8.78	0.9948	1.9792	0.005195	0.005223
9.16	0.9952	1.9728	0.005178	0.005204
11.01	0.9988	1.9735	0.005180	0.005187
12.07	0.9992	1.9510	0.005121	0.005126
		$T = 70$ °C		
1.08	0.9988	11.7265	0.030778	0.030850
2.05	0.9928	2.5658	0.006734	0.006785
3.04	0.9920	2.4304	0.006379	0.006432
4.08	0.9932	2.3929	0.006281	0.006325
5.28	0.9944	2.3814	0.006250	0.006287
6.66	0.9888	2.3145	0.006075	0.006145
7.25	0.9972	2.3216	0.006094	0.006112
8.24	0.9964	2.2867	0.006002	0.006025
8.78	0.9944	2.2772	0.005977	0.006012
9.16	0.9916	2.2579	0.005926	0.005987
11.01	0.9932	2.2064	0.005791	0.005832
12.07	0.9980	2.2056	0.005789	0.005802

increasing pH values above 3. The limited solubility of FS at higher pH values (>3) shows that FS is a favorable desilication agent. XRD analysis (see results in Table 7) has demonstrated that FS is stable at 30−70 °C.

Table 7. XRD Characterization of the Equilibrated Solids

temperature (°C)	M	pH value	equilibration time (h)	equilibrated solid phase
30	0.1−5.0 mol/L (NaOH)		10	FS
50	0.1−5.0 mol/L (NaOH)		10	FS
70	0.1−5.0 mol/L (NaOH)		10	FS
30	0.1−2.5 mol/L (NaCl)		10	FS
50	0.1−2.5 mol/L (NaCl)		10	FS
70	0.1−2.5 mol/L (NaCl)		10	FS
30	0.1−2.5 mol/L ($NaNO_3$)		10	FS
50	0.1−2.5 mol/L ($NaNO_3$)		10	FS
70	0.1−2.5 mol/L ($NaNO_3$)		10	FS
30	0.1−1.0 mol/L (NaOH) + 0.1−2.0 mol/L ($NaNO_3$)		10	FS
30		1−12	10	FS
50		1−12	10	FS
70		1−12	10	FS

4. Chemical Equilibrium Modeling

4.1. Modeling Procedure. 4.1.1. Equilibrium Relationships. The solubility equilibrium of FS in electrolyte solutions can be described by the following dissolution reaction:[25,26]

$$3CaO \cdot Al_2O_3 \cdot CaCl_2 \cdot 10H_2O(s) \leftrightarrow 4Ca^{2+} + 2Al(OH)_4^- + 2Cl^- + 4OH^- + 4H_2O \quad (1)$$

The thermodynamic equilibrium constant for reaction 1 is

$$K_{sp} = a_{Ca^{2+}}^4 a_{Al(OH)_4^-}^2 a_{Cl^-}^2 a_{OH^-}^4 a_{H_2O}^4 = (m_{Ca^{2+}}^4 \gamma_{Ca^{2+}}^4)(m_{Al(OH)_4^-}^2 \gamma_{Al(OH)_4^-}^2) \times (m_{Cl^-}^2 \gamma_{Cl^-}^2)(m_{OH^-}^4 \gamma_{OH^-}^4) a_{H_2O}^4 \quad (2)$$

where K_{sp} is the solubility product constant; $m_{Ca^{2+}}$, $m_{Al(OH)_4^-}$, m_{Cl^-}, and m_{OH^-} are the molal concentrations of the Ca^{2+} cation and $Al(OH)_4^-$, Cl^-, and OH^- anions in solution, respectively; $\gamma_{Ca^{2+}}$,$\gamma_{Al(OH)_4^-}$, γ_{Cl^-}, and γ_{OH^-} are the ion activity coefficients; and a_{H_2O} is the activity of water. In the Na−OH−Cl−NO_3−H_2O systems, the experimental FS solubility (expressed in units of mol/kg) is $s = \sum m_{Ca}$, i.e., s is taken as the sum of all "Ca"-containing species. This explains why the speciation modeling approach makes sense in this context. Table 8 provides a list with all species and their dissociation reactions considered in this system. As an example, the dissociation of $CaOH^+$ is given as follows:

$$CaOH^+ = Ca^{2+} + OH^- \quad (3)$$

The thermodynamic equilibrium constant for this reaction is

$$K_{CaOH^+} = \frac{(m_{Ca^{2+}}\gamma_{Ca^{2+}})(m_{OH^-}\gamma_{OH^-})}{m_{CaOH^+}\gamma_{CaOH^+}} \quad (4)$$

4.1.2. Thermodynamic Equilibrium Constant. To obtain the constants of aqueous speciation equilibria (e.g., $CaOH^+$), the standard-state thermodynamic parameters of each aqueous species are required. In the OLI software, two alternative

Table 8. Chemical Species and Their Speciation Reactions in the FS−NaOH−NaCl−$NaNO_3$−H_2O System

species	dissociation reactions
H_2O	$H_2O = H^+ + OH^-$
$CaCl_2(aq)$	$CaCl_2(aq) = CaCl^+ + Cl^-$
$CaCl^+$	$CaCl^+ = Ca^{2+} + Cl^-$
$CaOH^+$	$CaOH^+ = Ca^{2+} + OH^-$
$CaNO_3^+$	$CaNO_3^+ = Ca^{2+} + NO_3^-$
$HCl(aq)$	$HCl(aq) = H^+ + Cl^-$
$HNO_3(aq)$	$HNO_3(aq) = H^+ + NO_3^-$
$NaNO_3(aq)$	$NaNO_3(aq) = Na^+ + NO_3^-$
$AlO_2H_2Cl(aq)$	$AlO_2H_2Cl(aq) = Al^{3+} + 2OH^- + Cl^-$
$Al(OH)_2^+$	$Al(OH)_2^+ = AlOH^{2+} + OH^-$
$Al(OH)_3(aq)$	$Al(OH)_3(aq) = Al(OH)_2^+ + OH^-$
$Al(OH)_4^-$	$Al(OH)_4^- = Al(OH)_3(aq) + OH^-$
$AlOHCl^+$	$AlOHCl^+ = Al^{3+} + OH^- + Cl^-$
$AlOH^{2+}$	$AlOH^{2+} = Al^{3+} + OH^-$
$3CaO\cdot Al_2O_3\cdot CaCl_2\cdot 10H_2O(s)$	$3CaO\cdot Al_2O_3\cdot CaCl_2\cdot 10H_2O(s) = 4Ca^{2+} + 2Al(OH)_4^- + 2Cl^- + 4OH^- + 4H_2O$

Table 9. Parameters for Species Whose Equilibrium Has Been Calculated with the Aid of Eq 5[a]

species	*A*	*B*	*C*	*D*
$CaCl_2(aq)$	−46.242	14154.1	4.08507×10^{-4}	0.0
$CaCl^+$	2.40192	1871.39	-1.36144×10^{-2}	0.0
$HCl(aq)$	32.1499	−1328.3	-1.0083×10^{-1}	$9.668\,94 \times 10^{-5}$
$HNO_3(aq)$	4.469722	1555.311	1.589443×10^{-2}	0.0
$NaNO_3(aq)$	66.34443	−6971.921	-1.87637×10^{-1}	$1.562\,99 \times 10^{-4}$

[a] Data taken from the "public" databank of OLI.

methods are used to accomplish this task. The first method makes use of the revised HKF equation originally developed by Helgeson and co-workers,[27−31] whereas the second method makes use of an empirical equation of the form

$$\log_{10} K = A + \frac{B}{T} + CT + DT^2 \quad (5)$$

where *A*, *B*, *C*, and *D* are empirical parameters. *T* is the temperature (in Kelvin). Equation 5 may be applied to either solubility product constants or dissociation constants of solution complexes. Four empirical parameters are obtained via fitting to experimental solubility data. Table 9 lists the species whose *K* (equilibrium constants) are calculated by the OLI software with the help of eq 5. Table 10 lists the thermodynamic data of the relating species used by the OLI software to calculate equilibrium constants with the aid of the HKF equation.

Table 10. Thermochemical Data for the Main Species in the FS−NaOH−NaCl−$NaNO_3$−H_2O System[a]

species	$\bar{V}^0_{f,25}$ (cm^3/mol)	$\bar{C}^0_{f,25}$ (J/(K mol))	$\bar{S}^0_{f,25}$ (J/(K mol))	$\Delta\bar{H}^0_{f,25}$ (kJ/mol)	$\Delta\bar{G}^0_{f,25}$ (kJ/mol)
H^+	0	0	0	0	0
OH^-	−4.18	−137.19	−10.711	−229.99	−157.3
H_2O	18.1	75.3	69.95	−285.83	−237.19
$CaCl_2(aq)$	3.26	129.537	25.104	−883.08	−811.7
$CaCl^+$	5.74	73.0945	18.828	−705.46	−682.41
$CaOH^+$	45.0	89.445	−14.468	−764.378	−717.101
$HCl(aq)$	0	−31.8	105.28	−116.42	−95.111
$CaNO_3^+$	17.82	172.031	103.915	−748.233	−666.055
$HNO_3(aq)$	40.2	18	178.648	−189.99	−103.465
$NaNO_3(aq)$	36.71	515.343	279.219	−419.851	−367.565
$AlO_2H_2Cl(aq)$			−271.49	−116.403	−941.352
$Al(OH)_2^+$	17.79	−50.21	−43.05	−1000.0	−899.06
$Al(OH)_3(aq)$	20.39	−133.893	90.867	−1237.54	−1106.14
$Al(OH)_4^-$	50.18	100.805	109.684	−1500.93	−1305.13
$AlOHCl^+$			−118.3026	−934.1	−826.585
Na^+	1.11	−153.1	58.4086	−240.30	−261.881
Cl^-	17.79	−123.177	56.735	−167.08	−131.29
Ca^{2+}	18.06	−31.50	−56.48	−543.083	−552.79
Al^{3+}	44.4	−135.98	−325.1	−530.67	−483.7
NO_3^+	29	−68.614	146.935	−206.8	−110.894
$AlOH^{2+}$	28.2	55.229	−176.6	−767.02	−692.35

[a] The data are from the "public" databank of OLI.

4.1.3. Ion Activity Coefficient and Water Activity Relationships. It is clear from eqs 2 and 4 that determination of the FS solubility or the abundance of solution species requires the knowledge of the relevant ion activity coefficients and the activity of water. There are several types of coefficient models that may be used in this context.[20,32] However, the Bromley−Zemaitis activity coefficient model,[32] developed by Bromley[33] and empirically modified by Zemaitis,[20] is one of the models used by the OLI software. This model has been successfully used for electrolytes with concentrations of 0−30 M in the temperature range of 0−200 °C; hence, it is appropriate for the present system, which is <6 M in the temperature range of 20−200 °C. The Bromley−Zemaitis activity coefficient model for the case of cation *i* in a multicomponent electrolyte solution is expressed as follows:

$$\log \gamma_i = \frac{-AZ_i^2\sqrt{I}}{1+\sqrt{I}} + \sum_j \left\{ \frac{(0.06 + 0.6B_{ij})|Z_iZ_j|}{\left[1 + \left(1.5I/|Z_iZ_j|\right)\right]^2} + B_{ij} + C_{ij}I + D_{ij}I^2 \right\} \left(\frac{|Z_i| + |Z_j|}{2}\right)^2 m_j \quad (6)$$

where *j* indicates all anions in solution; *A* is the Debye−Huckel parameter; *I* is the ionic strength of the solution; *B*, *C*, and *D* are temperature-dependent empirical coefficients; and Z_i and Z_j are the cation and anion charges, respectively. $B_{ij} = B_{1ij} + B_{2ij}T + B_{3ij}T^2$ (where *T* is the temperature (in Celsius)), and the other coefficients *C* and *D* have similar forms of temperature dependence. For the activity coefficient of an anion, the subscript *i* represents that anion and the subscript *j* then represents all cations in the solution. Each ion pair is described with this nine-parameter equation. The nine parameters are determined by regression of the electrolyte solution properties, such as solubility data.

In the case of neutral aqueous species, e.g., $CaCl_2^0$, the Bromley−Zemaitis model (eq 6) cannot be used. In this case, the expression proposed by Pitzer[34] is used to obtain the activity coefficient:

$$\ln \gamma_{aq} = 2\beta_{0(m-m)} + 2\beta_{1(m-s)}m_s \quad (7)$$

where $\beta_{0(m-m)}$ is the adjustable parameter for molecule−molecule interactions, $\beta_{1(m-s)}$ represents the adjustable parameter for molecule−ion interactions, and m_s is the concentration of the neutral species.

Finally, for the activity of water in a multicomponent system, the formulation proposed by Meissner and Kusik[35] is adopted in the OLI thermodynamic framework:

$$\log(a_w)_{mix} = \sum_i \sum_j X_i Y_j \log(a_w^0)_{ij} \quad (8)$$

where a_w^0 is the hypothetical water activity of pure electrolyte ij (where i is an odd number for all cations and j is an even number for all anions), X_i represents cationic fraction ($X_i = I_i/I_c$), and Y_j represents the anionic fraction ($Y_j = I_j/I_a$).

4.2. K_{sp} Determination of FS. FS was not found in the current OLI software. Therefore, a new databank was created, which is called "private", in which FS was added successfully. To calculate the solubility of FS, the solubility product of FS is required. Initially, the solubility of FS in pure water at various temperatures was used to obtain the solubility product of FS (refer to eq 5). The adopted equation for the solubility product constant of FS is given below:

$$\log_{10} K_{sp} = 14.16 - \frac{15660}{T} + 0.1871T - 0.0004833T^2 \quad (9)$$

4.3. Solubility Estimation by OLI. The parameters in eq 9 were added into the newly established "private" databank. With the aid of eq 9, the solubility values of FS in the $Na-OH-Cl-NO_3-H_2O$ systems or at different pH values were obtained using the default database of OLI. Both sets of data (the results obtained using the default database of OLI and experimental) are plotted in Figure 6 for the case of the solubility of FS in NaOH solutions. As can be seen, a relatively large deviation of the results obtained using the default database of OLI from experiments is observed. Figures 7 and 8 provide further comparisons between the results obtained using the default database of OLI and the experiments in the case of FS solubility in NaCl and $NaNO_3$ solutions. As can be seen, at low temperatures and salts (NaCl or $NaNO_3$) concentrations, the results obtained using the default database of OLI are satisfactory, whereas at temperatures above 50 °C and salts concentrations above 1 mol/kg, the deviation becomes significant. Similarly, in mixed NaOH + $NaNO_3$ solutions, the deviation is relatively large (see Figure 9). In addition, a comparison of experimental results and the results obtained using the default database of OLI at different pH values is presented in Figure 10. A significant deviation is observed at higher pH values (>7) in the temperature range of 30−70 °C.

4.4. Model Parameterization. With the purpose of improving OLI's prediction capability, in regard to FS solubilities in the $Na-OH-Cl-NO_3-H_2O$ systems or at various pH values, new model parameters were determined via the regression of the solubility data of FS in water and in single electrolyte solutions, such as NaOH, NaCl, and $NaNO_3$, under atmospheric pressure. In this regression, the model parameters are obtained by minimizing the sum of squared deviations between the experimental and calculated values of solubility of FS. In particular, the parameters of two model equations were scrutinized and modified (when necessary): the Bromley−Zemaitis activity coefficient model parameters in eq 6 and the empirical parameters in an equilibrium constant relationship (eq 5). The main aqueous species or ions present in the FS−NaOH−$NaCl-NaNO_3-H_2O$ system are listed in Table 8. Among these possible ion pairs, only the Bromley−Zemaitis parameters for three pairs, namely, $Ca^{2+}-OH^-$, $CaOH^+-OH^-$, and $CaCl^+-OH^-$, were regressed with the new model parameters, with all other ion pairs kept the same as in OLI's default databank. The newly determined parameters are listed in Table 11. These ion pairs were selected because they were thought to directly impact on the solubility of FS. The best fit was obtained when the dissociation constant of the $CaOH^+$ ion was expressed with the aid of eq 5 and not by the HKF method. The adopted equation for the dissociation constant of $CaOH^+$ is given below:

Table 11. Newly Regressed Bromley−Zemaitis Model Parameters for $Ca^{2+}-OH^-$, $CaOH^+-OH^-$, and $CaCl^+-OH^-$ Interactions

	Value		
parameter	$Ca^{2+}-OH^-$	$CaOH^+-OH^-$	$CaCl^+-OH^-$
B1	2.271×10^{-2}	6.885×10^{-3}	-1.199×10^{-2}
B2	4.115×10^{-4}	2.412×10^{-4}	-9.413×10^{-5}
B3	5.217×10^{-7}	1.005×10^{-6}	-2.027×10^{-7}
C1	-2.598×10^{-3}	-3.4×10^{-3}	-2.788×10^{-3}
C2	-6.399×10^{-6}	-2.373×10^{-5}	-5.367×10^{-5}
C3	6.619×10^{-7}	-1.747×10^{-7}	-1.537×10^{-6}
D1	-4.728×10^{-5}	-4.902×10^{-6}	-2.351×10^{-5}
D2	-6.135×10^{-7}	-2.242×10^{-7}	-7.979×10^{-7}
D3	5.223×10^{-8}	-1.274×10^{-7}	-1.203×10^{-6}

$$\log_{10} K_{CaOH^+} = -2.954 + \frac{394.4}{T} + 0.008718T - 7.165 \times 10^{-6}T^2 \quad (10)$$

By obtaining the new model parameters (Table 11 and eq 10) simultaneously, the comparisons between the regressed model results and the experimental results were provided. As can be seen from Figure 3, the regression results accurately fit the experimental solubility of FS in water with an average deviation of ±0.00012 mol/kg H_2O for 20 points. In the case of NaOH, the regressed model results (Figure 6) are roughly consistent with the experimental results with an average deviation of ±0.000053 mol/kg H_2O. In the case of NaCl and $NaNO_3$, the fitted results (Figures 7 and 8) are in good agreement with the experimental results.

4.5. Test of the Model. Having successfully modeled the solubility data of FS in water or in single electrolyte solutions, the new model parameters were subsequently tested by comparing model predictions with experimental data. To accomplish this task, the newly obtained Bromley−Zemaitis parameters shown in Table 11 and the new parameters of the dissociation equilibrium constant of $CaOH^+$ ion (eq 10) were added into the newly established "private" databank. The model equipped with the new parameters was tested by comparing the predicted values to the solubility data of FS in the mixed NaOH + $NaNO_3$ solutions at 30 °C. Excellent agreement between the obtained parameters predictions and experimental data (Table 5) is observed in Figure 9. Also, the obtained parameters were further tested by comparing the predicted values to the solubility data of FS at various pH values. As can be seen from Figure 10, equally good agreement is observed between the experimental data (Table 6) and the parameter predictions that were obtained.

To test the applicability of the newly obtained parameters, a comparison of calculated values by OLI's existing model and predictions by the newly developed model for the solubility of $Ca(OH)_2$ in 0−1.0 mol/kg NaOH solutions at 30 °C is also presented in Figure 11. As can be seen, the solubility values by both methods are very close, indicating the reliability of the obtained parameters.

4.6. Use of the Model. OLI's StreamAnalyzer 3.0 program, which was equipped with the new model parameters developed

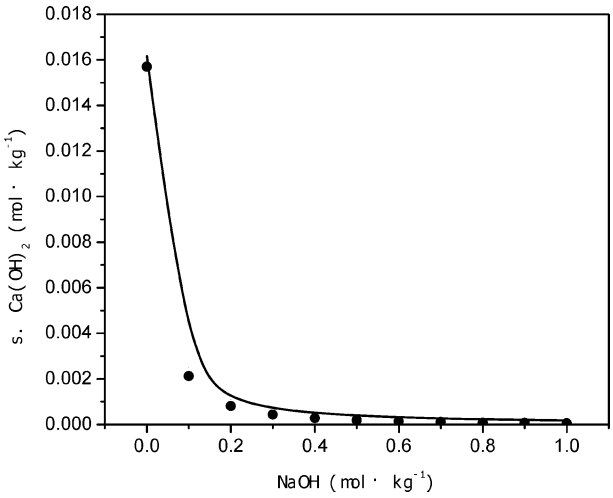

Figure 11. Comparison of the solubility of $Ca(OH)_2$ in NaOH solutions at 30 °C. Points present the predicted values by the obtained parameters; the solid lines represent the values calculated using the OLI existing model.

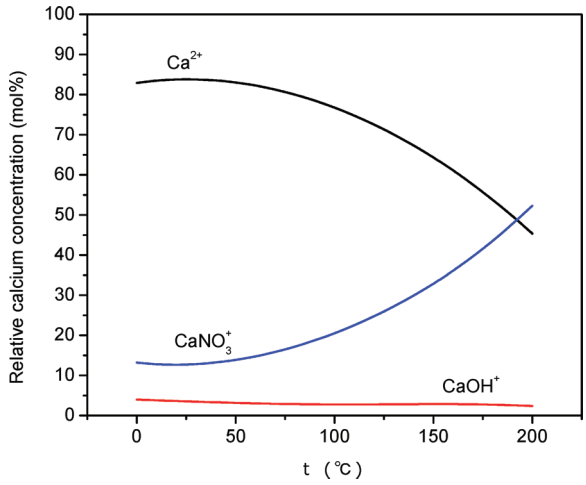

Figure 12. Calcium speciation, as a function of temperature, for a FS-saturated solution containing 0.5 m NaOH and 0.5 m $NaNO_3$.

in this work, was used to analyze the temperature and concentration effects on calcium species distribution.

4.6.1. Temperature Effects. Figure 12 shows the relative concentration of calcium species (Ca^{2+}, $CaOH^+$, and $CaNO_3^+$) in FS-saturated solutions containing 0.5 m NaOH and 0.5 m $NaNO_3$, as a function of temperature. In this case, the solubility of FS is equal to the total concentration of these calcium species in the solution. It is obvious that the relative concentration of $CaNO_3^+$ first increases smoothly with increasing temperature and then increases sharply with increasing temperature over 80 °C, while the relative concentration of Ca^{2+} has the reverse trend against $CaNO_3^+$ in the temperature range of 20−200 °C. The relative concentrations of $CaNO_3^+$ and Ca^{2+} are 12.8% and 83.8%, respectively, at 30 °C, but 52.3% and 45.4%, respectively, at 200 °C. The $CaOH^+$ species is present in <4% of the total calcium concentration within the temperature range of 20−200 °C.

4.6.2. Concentration Effects. The relative concentration of calcium species in the system containing FS, NaOH, $NaNO_3$, and H_2O, as a function of $NaNO_3$ concentration, is shown in Figure 13 for the case of 0.5 m NaOH. It can be observed that the relative concentration of $CaNO_3^+$ first increases rapidly with increasing $NaNO_3$ concentration and then increases insignificantly with further increasing $NaNO_3$ concentration. Simultaneously, the relative concentration of Ca^{2+} has a reverse trend against $CaNO_3^+$ at 30 °C up to 5 mol/kg $NaNO_3$, while the relative concentration of $CaOH^+$ consistently decreases smoothly.

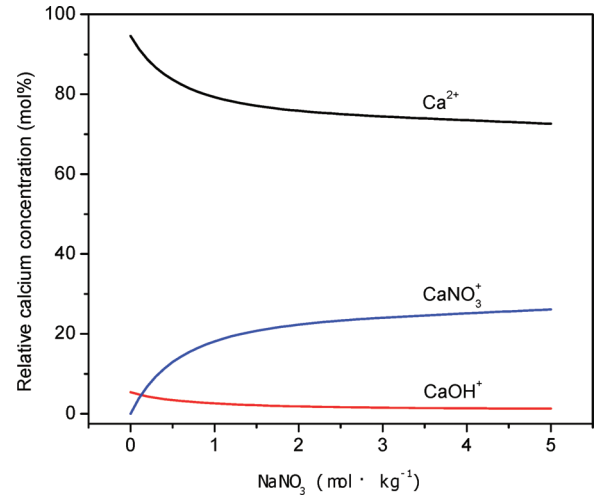

Figure 13. Calcium speciation at 30 °C, as a function of concentration, for a FS-saturated $NaNO_3$ solution with 0.5 m NaOH.

5. Conclusions

The solubility of Friedel's salt (FS) in the Na−OH−Cl−NO_3−H_2O systems or at various pH values has been measured in the temperature range of 20−200 °C, using the isothermal dissolution method. The solubility of FS in all cases investigated was found to increase with temperature, with the exception of FS in water. The solubility of FS in water initially increases, passing a maximum, and then decreases sharply with further increasing temperature. The solubility in NaOH initially decreases sharply and then decreases smoothly with a further increase in the concentration, because of the common ion effect of added OH^-. The addition of $NaNO_3$ results in a significant increase in the solubility because of the formation of calcium nitrate complexes. It was found that the solubility in NaCl decreases sharply, because of the common ion effect of added Cl^-. The solubility initially decreases sharply and then decreases smoothly with increasing pH values greater than 3. X-ray diffraction (XRD) and scanning electron microscopy (SEM) showed that FS is stable in all cases.

The experimentally measured solubility data were successfully modeled via the OLI platform based on the Bromley−Zemaitis activity coefficient model. The empirical parameters of K_{sp} for FS were obtained by the regression of the solubility data in H_2O at various temperatures using the OLI regression module and then added into a new databank called "private". Subsequently, OLI's StreamAnalyzer 3.0 program, with this private databank, was used to estimate the FS solubility in NaOH, NaCl, $NaNO_3$, and mixed NaOH + $NaNO_3$ solutions or at different pH values with limited success. The source of deviation of OLI's estimation from the experimental data was traced to the Bromley−Zemaitis model parameters for Ca^{2+}−OH^-, $CaOH^+$−OH^-, and $CaCl^+$−OH^- ion pairs, as well as the dissociation constant of $CaOH^+$. A new set of model parameters was determined via regression of solubility data of FS in water and in single electrolyte solutions. The new model parameters yielded a highly improved model capable of predicting the solubility of FS in mixed NaOH + $NaNO_3$ solutions or at various pH values. Finally, with the aid of the model, the concentration and temperature effects on calcium species distribution were successfully analyzed. It was found that

temperature has a stronger effect on the distribution of calcium species ($CaNO_3^+$ and Ca^{2+}) than concentration.

Acknowledgment

The support of the National Basic Research Program of China (973 Program, No. 2007CB613501, and No. 2009CB219904) and the National Natural Science Foundation of China (Grant No. 21076212) is gratefully acknowledged.

Literature Cited

(1) Authier-Martin, M.; Forte, G.; Ostap, S.; See, J. The mineralogy of bauxite for producing smelter grade alumina. *JOM* **2001**, *53*, 36–40.

(2) Tizon, E.; Clerin, P.; Cristol, B. Effect of predesilication and digestion conditions on silica level in Bayer liquor. In *Light Metals 2004*; Tabereaux, A. T., Ed.; The Minerals, Metals & Materials Society (TMS): Warrendale, PA, 2004; pp 9−14.

(3) Addai-Mensah, J.; Jones, J.; Zbik, R.; Gerson, A. Sodium aluminosilicates scale formation on steel substrates: Experimental design and assessment of fouling behavior. In *Light Metals 2003*; Paul, N. C., Ed.; The Minerals, Metals & Materials Society (TMS): Warrendale, PA, 2003; pp 25−34.

(4) Armstrong, J. A.; Dann, S. E. Investigation of zeolite scales formed in the Bayer process. *Microporous Mesoporous Mater.* **2000**, *41*, 89–97.

(5) Miyata, S. Anion-exchange properties of hydrotalcite-like compounds. *Clays Clay Miner.* **1982**, *31*, 305–311.

(6) Ma, J. Y.; Li, Z. B.; Zhang, Y.; Demopoulos, G. P. Desilication of sodium aluminate solution by Friedel's salt (FS: $3CaO\cdot Al_2O_3\cdot CaCl_2\cdot 10H_2O$). *Hydrometallurgy* **2009**, *99*, 225–230.

(7) Suryavanshi, A. K.; Scantlebury, J. D.; Lyon, S. B. Mechanism of Friedel's salt formation in cements rich in tricalcium aluminate. *Cem. Concr. Res.* **1996**, *26*, 717–727.

(8) Birnin-Yauri, U. A.; Glasser, F. P. Friedel's salt, $Ca_2Al(OH)_6(Cl,OH)$: Its solid solutions and their role in chloride binding. *Cem. Concr. Res.* **1998**, *28*, 1713–1723.

(9) Gougar, M. L. D.; Scheetz, B. E.; Roy, D. M. Ettringite and C−S−H Portland cement for waste ion immobilization: A review. *Waste Manage.* **1996**, *16*, 295–303.

(10) Walcarius, A.; Lefevre, G.; Rapin, J. P. Voltammetric detection of iodide after accumulation by Friedel's salt. *Electroanalysis* **2001**, *13*, 313–320.

(11) Qian, G. R.; Cao, Y. L.; Chui, P.; Tay, J. Utilization of MSWI fly ash for stabilization/solidification of industrial waste sludge. *J. Hazard. Mater.* **2006**, *129*, 274–281.

(12) Dai, Y. C.; Qian, G. R.; Cao, Y. L.; Chi, Y.; Xu, Y. F.; Zhou, J. Z.; Liu, Q.; Xu, Z. P.; Qiao, S. Z. Effective removal and fixation of Cr(VI) from aqueous solution with Friedel's salt. *J. Hazard. Mater.* **2009**, *170*, 1086–1092.

(13) Azimi, G.; Papangelakis, V. G.; Dutrizac, J. E. Modelling of calcium sulphate solubility in concentrated multi-component sulphate solutions. *Fluid Phase Equilib.* **2007**, *260*, 300–315.

(14) Azimi, G.; Papangelakis, V. G.; Dutrizac, J. E. Development of an MSE-based chemical model for the solubility of calcium sulphate in mixed chloride−sulphate solutions. *Fluid Phase Equilib.* **2008**, *266*, 172–186.

(15) Azimi, G.; Papangelakis, V. G.; Dutrizac, J. E. Development of a chemical model for the solubility of calcium sulphate in zinc processing solutions. *Can. Metall. Q.* **2010**, 49.

(16) Azimi, G.; Papangelakis, V. G. Thermodynamic modelling and experimental measurement of calcium sulphate solubility in complex aqueous solutions. *Fluid Phase Equilib.* **2010**, *290*, 88–94.

(17) Azimi, G.; Papangelakis, V. G. The solubility of gypsum and anhydrite in simulated laterite pressure leach solutions up to 250 °C. *Hydrometallurgy* **2010**, *102*, 1–13.

(18) Li, Z. B.; Demopoulos, G. P. Development of an improved chemical model for the estimation of $CaSO_4$ solubilities in the $HCl-CaCl_2-H_2O$ system up to 100 °C. *Ind. Eng. Chem. Res.* **2006**, *45*, 2914–2922.

(19) Li, Z. B.; Demopoulos, G. P. Speciation-based chemical model of $CaSO_4$ solubility in the H + Na + Ca + Mg + Al + Fe(II) + Cl + SO_4 + H_2O system. *Ind. Eng. Chem. Res.* **2007**, *46*, 6385–6392.

(20) Zemaitis, J. F. Predicting vapor−liquid equilibria in multicomponent aqueous solutions of electrolytes. In *Thermodynamics of Aqueous Systems with Industrial Applications*; Newman, S. A., Barner, H. E., Klein, M., Eds.; ACS Symposium Series 133; American Chemical Society: Washington, DC, 1980; p 227.

(21) Cheng, W. T.; Li, Z. B. Controlled supersaturation precipitation of hydromagnesite for the $MgCl_2-Na_2CO_3$ system at elevated temperatures: Chemical modelling and experiment. *Ind. Eng. Chem. Res.* **2010**, *49*, 1964–1974.

(22) Hefter, G. T.; Tomkins, R. P. T. *The Experimental Determination of Solubilities*; John Wiley & Sons, Ltd.: Chichester, U.K., 2003.

(23) Templeton, C. C. The solubility of calcium sulfate in aqueous solutions of sodium nitrate between 573 and 623 K. *J. Chem. Thermodyn.* **1976**, *8*, 99–100.

(24) Marshall, W. L.; Slusher, R. The ionization constant of nitric acid at high temperatures from solubilities of calcium sulfate in HNO_3-H_2O, 100−350 °C; activity coefficients and thermodynamic functions. *J. Inorg. Nucl. Chem.* **1975**, *37*, 1191–1202.

(25) Bothe, J. V.; Brown, P. W. PhreeqC modeling of Friedel's salt equilibria at 23 ± 1 °C. *Cem. Concr. Res.* **2004**, *26*, 1057–1063.

(26) Suryavanshi, A. K.; Swamy, R. N. Stability of Friedel's salt in carbonated concrete structural elements. *Cem. Concr. Res.* **1996**, *26*, 729–741.

(27) Shock, E. L.; Helgeson, H. C. Calculation of the thermodynamic and transport properties of aqueous species at high pressures and temperatures: Correlation algorithms for ionic species and equation of state predictions to 5 kb and 1000 °C. *Geochim. Cosmochim. Acta* **1988**, *52*, 2009–2036.

(28) Helgeson, H. C.; Kirkham, D. H.; Flowers, G. C. Theoretical prediction of the thermodynamic behavior of aqueous electrolytes at high pressures and temperatures. IV. Calculation of activity coefficients, osmotic coefficients, and apparent molar and standard and relative partial molar properties to 600 °C and 5 kb. *Am. J. Sci.* **1981**, *281*, 1249–1516.

(29) Tanger, J. C.; Helgeson, H. C. Calculation of the thermodynamic and transport properties of aqueous species at high pressures and temperatures: Revised equation of state for the standard partial molar properties of ions and electrolytes. *Am. J. Sci.* **1988**, *288*, 19–98.

(30) Shock, E. L.; Helgeson, H. C.; Sverjensky, D. A. Calculation of the thermodynamic and transport properties of aqueous species at high pressures and temperatures: Standard partial molar properties of inorganic neutral species. *Geochim. Cosmochim. Acta* **1989**, *53*, 2157–2183.

(31) Shock, E. L.; Sassani, D. C.; Willis, M.; Sverjensky, D. A. Inorganic species in geologic fluids: Correlation among standard molar thermodynamic properties of aqueous ions and hydroxide complexes. *Geochim. Cosmochim. Acta* **1997**, *61*, 907–950.

(32) Rafal, M.; Berthold, J. W.; Scrivner, N. C.; Grise, S. L. Models for electrolyte solutions. In *Models for Thermodynamic and Phase Equilibria Calculations*; Sandler, S. I., Ed.; Marcel Dekker: New York, 1994.

(33) Bromley, L. A. Thermodynamic properties of strong electrolytes in aqueous solutions. *AIChE J.* **1973**, *19*, 313–320.

(34) Pitzer, K. S. *Activity Coefficients in Electrolyte Solution*; CRC Press: Boca Raton, FL, 1991.

(35) Meissner, H. P.; Kusik, C. L. Aqueous solutions of two or more strong electrolytes: Vapor pressure and solubilities. *Ind. Eng. Chem. Process Des. Dev.* **1973**, *12*, 205–208.

Received for review May 5, 2010
Revised manuscript received July 26, 2010
Accepted August 9, 2010

IE101028C